

## CHANGES IN MAGNETIC DOMAIN STRUCTURE OF MARAGING STEEL STUDIED BY MAGNETIC FORCE MICROSCOPY

**Miroslaw Bramowicz<sup>1</sup>, Sławomir Kulesza<sup>2</sup>, Grzegorz Mrozek<sup>1</sup>**

<sup>1</sup> Chair of Materials and Machinery Technology

<sup>2</sup> Chair of Relativistic Physics

University of Warmia and Mazury in Olsztyn

Received 29 September 2014, accepted 19 November 2014, available on line 24 November 2014.

**K e y w o r d s:** Maraging Steel, Magnetic Force Microscopy, Fractal Analysis.

### Abstract

The paper presents results on whether and how the magnetic domain structure in maraging steel undergoes any change due to the aging process. It continues the works on application of correlation methods and fractal analysis into studies of magnetic properties of various steel alloys using Scanning Probe Microscopy. It is aimed at verifying the usefulness of the structure function for description of spatial changes in shape and orientation of magnetic domains, and the magnitude of magnetic stray field affected by the heat treatment.

Obtained results suggest that despite vanishing magnetic tip-surface interaction, and hence vanishing magnetic stray field, magnetic domains remain nearly perfectly isotropic although randomly oriented. Similar to isotropic real surfaces, the fractal dimension of the magnetic domains turns out to be independent of the structural changes induced by the aging process, whereas the topography is found to vary within order of magnitude along with changes in the magnetic stray field. After all, obtained results lead to conclusion that the aging process leaves its fingerprints in the structure of the steel alloys, which can be studied using numerical analysis of images of magnetic interactions between vibrating tip and the stray field.

## Introduction

In the seventies, precipitation hardening steels gained large attention as attractive construction materials renowned for their advantageous properties, for example: high mechanical strength (up to 2.5 GPa), good plasticity, low susceptibility to cracking, and others (BOJARSKI, MATYJA 1983, DOBRZAŃSKI 2002). Having good mechanical properties, these steels were initially used in

---

Correspondence: Miroslaw Bramowicz, Katedra Technologii Materiałów i Maszyn, Uniwersytet Warmińsko-Mazurski, ul. Oczapowskiego 11, 10-719 Olsztyn, phone: 48 89 523 38 55, e-mail: miroslaw.bramowicz@uwm.edu.pl

the aerospace, aviation as well as military industries, but then they were also recognized good tool materials. Among them, H15K20M3JPr (X2CoCrMoAl20-15-3 according to PN-EN 10027-1) steel was distinguished as it possessed not only high mechanical strength, and impact toughness ( $Rm = 1.2$  GPa,  $KCU = 90$  J/cm<sup>2</sup> after aging procedure), but also significant corrosion resistance. Although in the second half of the eighties, due to scarce natural resources, and high price of cobalt, it was partly replaced by several substitutes, but now it is becoming popular again as a material investigated in fundamental research using modern scientific methods and instruments.

This paper continues the works on application of correlation methods to study magnetic properties of steels from Scanning Probe Microscope (SPM) images, which were presented previously (BRAMOWICZ, KULESZA 2013, BRAMOWICZ et al. 2014). It is aimed at verifying fractal nature of magnetic domains derived from SPM images using autocorrelation functions of the first and second orders. Recorded SPM signal reflects magnetic interaction between the field emitted from the surface, and the magnetized tip. As mentioned previously, this study is devoted to analysis of H15K20M3JPr (X2CoCrMoAl20-15-3) steel subjected to the aging process at various temperatures. Phase precipitates caused by the aging are expected to influence the spatial structure of magnetic domains, and hence the magnitude of the stray magnetic field. Observed changes are characterized using the following parameters: root mean square deviation of the phase shift between forced cantilever oscillation and the driving signal ( $Sq$ ), fractal dimension ( $D_{ACF}$ ), and the topothesy ( $K_{ACF}$ ). The fractal parameters ( $D_{ACF}$ , and  $K_{ACF}$ ) are determined using the algorithm described elsewhere (BRAMOWICZ et al. 2014). First of all, the 1-dimensional autocorrelation function  $R(\tau)$  (ACF) is to be computed from the profiles of the magnetic interaction map  $z(x)$  according to:

$$R(\tau) \langle (z(x) - \langle z(x) \rangle) \cdot (z( + \tau) - \langle z(x) \rangle) \rangle \quad (1)$$

where:

$\tau$  – is the discrete spatial lag along the scan axis, whereas  $\langle \dots \rangle$  denotes the mean value. Having the ACF, the structure function  $S(\tau)$  (SF) can be calculated in the next step using the relation given by SAYLES and THOMAS (1978):

$$S(\tau) = 2 \cdot (Sq^2 - R(\tau)) \quad (2)$$

Figure 1 shows an exemplary graph of the structure function obtained in this way. Note the two characteristic parts of the  $S(\tau)$  curve drawn in a log-log plot delimited by the so-called corner frequency  $\tau_c$ , which establishes the minimum spatial lag between uncorrelated points on the map of magnetic

interactions. In the first range ( $\tau \ll \tau_c$ ), the structure function obeys the power law given by:

$$S(\tau) \propto \tau^{2(2-D_{\text{ACF}})} \quad (3)$$

In the second range ( $\tau \gg \tau_c$ ), the ACF asymptotically goes to zero, and hence the SF is approaching a constant value:

$$S(\tau) \approx 2 \cdot S_q^2 \quad (4)$$

On the whole, the SF curve can be described by the equation:

$$S(\tau) = K \tau^{2(2-D_{\text{ACF}})} \quad (5)$$

where:

$K$  – is the topothesy expressed according to WU (2002):

$$K = \frac{\pi G^{2(D_{\text{ACF}}-1)}}{2\Gamma(5 - 2D_{\text{ACF}} \sin[\pi(2 - D_{\text{ACF}})])} \quad (6)$$

where:

$\Gamma$  – is the Euler's gamma function.

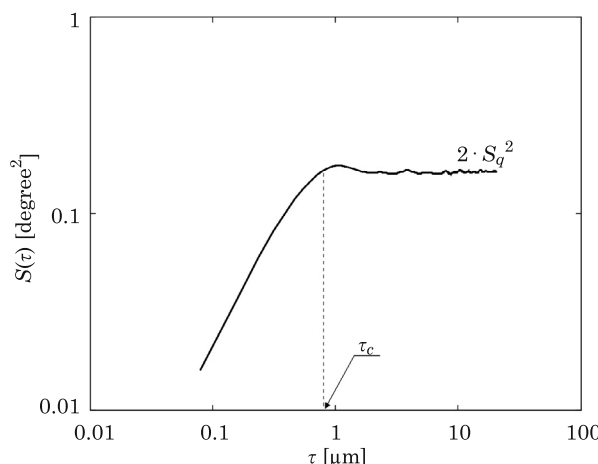


Fig. 1. Exemplary plot of the profile structure function

## **Experiment**

Heat-treated samples of dimensions  $25 \times 45 \times 5$  mm were cut out of forged steel rod with a rectangular cross section of dimensions 100 mm by 100 mm. The heat treatment involved supersaturation at 1050°C for 30 min followed by recurrent aging cycles at increasing temperatures (500, 550, and 600°C, respectively). The aim of aging was to induce microstructural transitions within the steel responsible for changes in the magnetic domain structures, which were further studied using metallography, microhardness measurements, as well as Magnetic Force Microscopy (MFM), i.e. one of SPM modes.

Prior to metallographic examination, samples were polished, and etched in a Marble reagent. The measurements were carried out using Olympus XC-70 microscope with digital image acquisition. In turn, HV0.1 microhardness measurements were done using Innovatest 413D instrument in accordance with ISO 6507-1 standard. Magnetic domains were studied using Multimode 8 Scanning Probe Microscope (Bruker) with Nanoscope V controller (Bruker). In order to enhance the magnetic interaction, the scanning probes (MESP from Bruker, with 35 nm tip radius, and 400 Oe coercivity) were magnetized using strong permanent magnet prior to the measurements. The measurements were carried out in a two-pass mode, which was described in details elsewhere (BRAMOWICZ, KULESZA 2014), passing the scanning probe with the lift height 100 nm above the surface.

## **Results and discussion**

Microstructural investigations of a sample in a supersaturated state reveal coarse microstructure of the alloy containing small non-metallic inclusions. This microstructure, together with microhardness as well as magnetic domain pattern, is significantly changed due to the aging. More specifically, the alloy initially exhibits coarse, polygonal structure of supersaturated austenite, but after the heat treatment at 500, 550 i 600°C, characteristic twins appear in its structure. The twins with small precipitates of intermetallic phases are located mostly in the austenite grain boundaries. It can be also seen coagulation of precipitated phases, which progressively increases with increasing aging temperature. Discussed changes in microstructure caused by the heat treatment are shown in Figure 2.

Precipitation of intermetallic phases from supersaturated solution significantly influences structural composition of the alloy, and hence its microhardness, as seen in Figure 3. On the other hand, microstructural changes in the

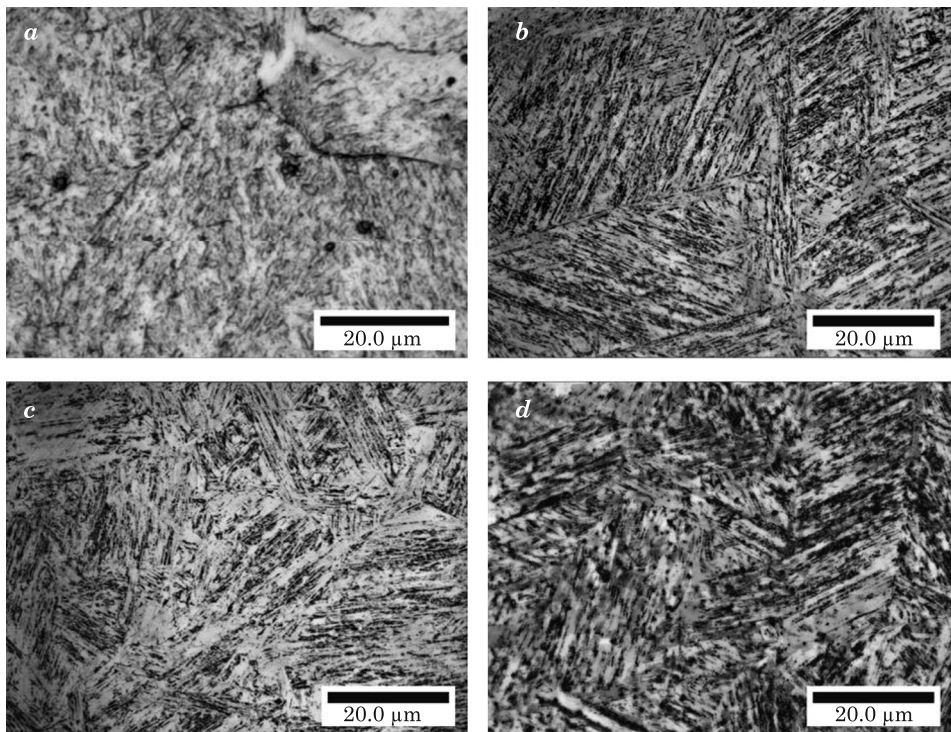


Fig. 2. Microstructure of X2CoCrMoAl20-15-3 steel in a supersaturated state (a), and after aging at, respectively: b) 500°C, c) 550°C, d) 600°C

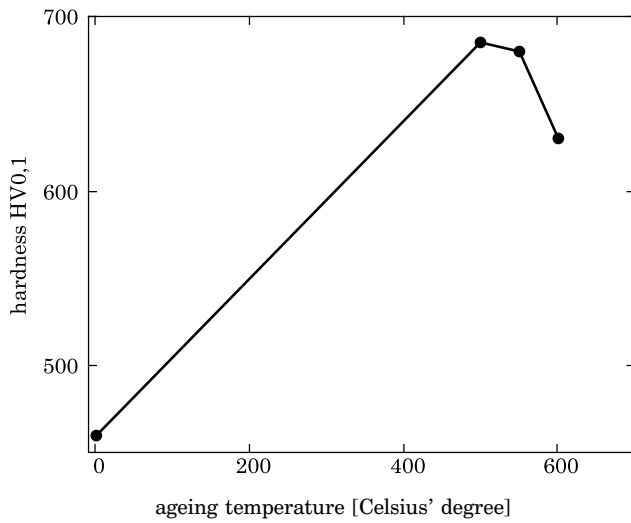


Fig. 3. Changes in microhardness due to the aging process

alloy's lattice are likely to modify the pattern of magnetic domains together with its characteristic parameters.

Figure 4 shows the images of magnetic stray field over the samples surface. Obtained results clearly indicate vanishing phase shifts between vibrating cantilever and the driving signal, which are due to decreasing tip-surface magnetic interaction. In addition, magnetic domains are becoming blurry pointing at discontinuities in magnetic material associated with precipitations of non-magnetic phases. The latter observation is supported by decreasing root-mean-square deviations of the phase shifts shown in Figure 5a.

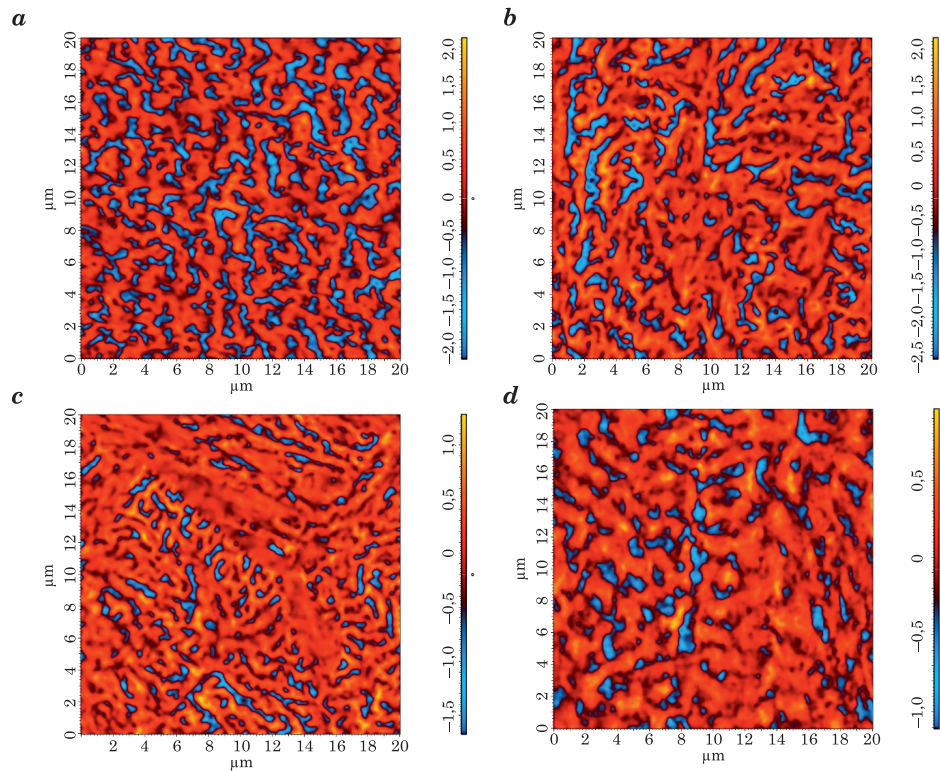


Fig. 4. Magnetic domains in X2CoCrMoAl20-15-3 steel in a supersaturated state *a*, and after the aging at, respectively: *b*) 500°C, *c*) 550°C, *d*) 600°C

Figure 5b, and 5c show results of the fractal analysis that investigates self-affine properties of the magnetic domains. First of all, domains observed in Figure 4 exhibit random orientation, that is, they look nearly identical in all directions. In order to confirm this suggestion, the measure of anisotropy is estimated, the so-called anisotropy ratio  $S_{tr}$ , according to method described elsewhere (BRAMOWICZ, KULESZA 2013). Basically, anisotropy ratio is defined

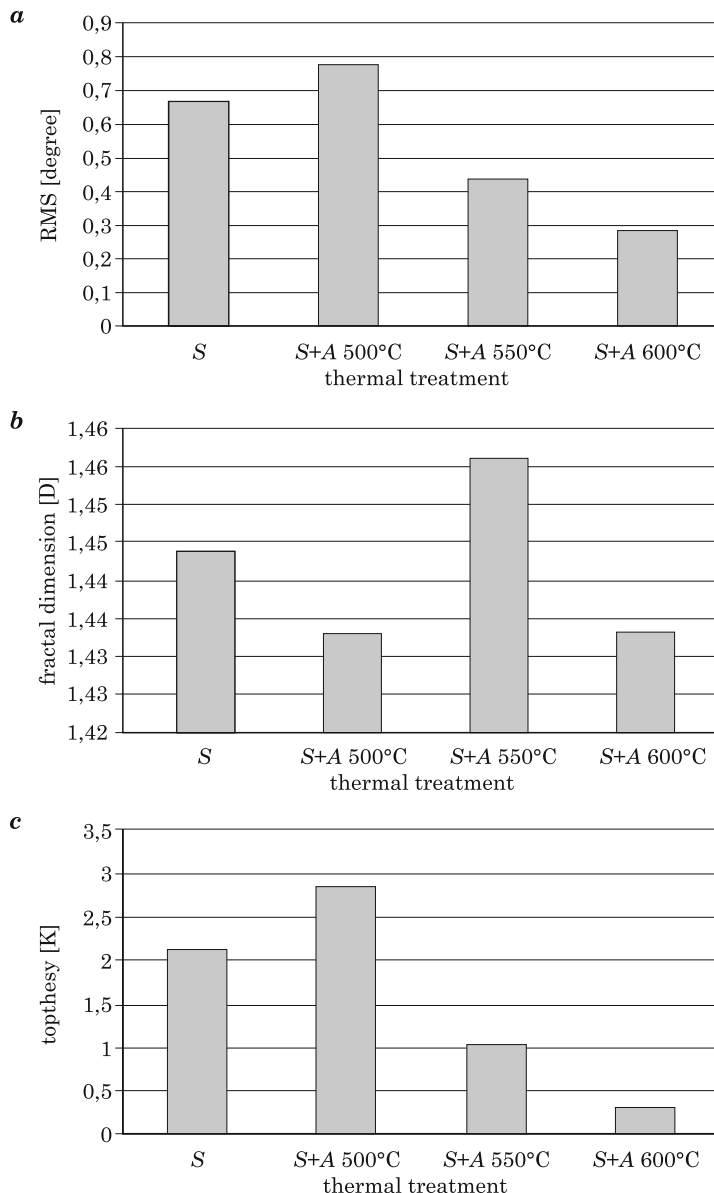


Fig. 5. Influence of the thermal treatment on: a) the phase shift between cantilever oscillations and the driving piezo signal (RMS values), b) fractal dimension DACF, c) topohesy K

as a ratio between minimum and maximum autocorrelation decay lengths, along which the autocorrelation function decreases from  $R = 1.0$  down to  $R = 0.2$  (MAINSAH et al. 2001):

$$0 < S_{tr} = \left. \frac{\tau_{\min}}{\tau_{\max}} \right|_{R=1 \rightarrow 0.2} \leq 1 \quad (7)$$

where:

$\tau_{\min}$  and  $\tau_{\max}$  – the lengths of the decay of the autocorrelation function from  $R = 1.0$  down to 0.2 along main anisotropy directions  $a_1$  and  $a_2$ , respectively. Anisotropy ratio computed for domain images in Figure 4 is found at, respectively: 0.86, 0.86, 0.84, and 0.84. After all, such  $S_{tr}$  values (close to 1.0) confirm high isotropicity, and almost no influence of the aging process on the domain orientation.

Similarly, Figure 5b shows that the heat-treatment also has insignificant influence on the fractal dimension  $D_{ACF}$  that varies in the range from 1.43 to 1.46, that is within 2 per cent. On the other hand, Figure 5c exhibits large changes in the topography due to the aging process, which falls in the range from 0.25 up to 3, i.e. varies within order of magnitude under the treatment. In general, these observations are in good agreement with previous findings on the fractal properties of real surfaces, according to which in isotropic specimens fractal dimension remains constant, but the topography is sensitive to structural changes.

## Conclusions

The following conclusions can be drawn from performed measurements:

1. Fractal analysis together with fractal parameters are useful tools for mathematical description of evolution of magnetic domains in terms of their shape, orientation, and the magnitude of the magnetic stray field similar to surfaces of real 3-dimensional objects.
2. Changes in topography are proportional to those in magnetic tip-surface interaction.
3. Changes in magnetic tip-surface interaction have no influence on the fractal dimension  $D_{ACF}$  unless significant changes in the domains' structure occur.

## References

- BOJARSKI Z., MATYJA P. 1983. *Stale maraging – tworzywo narzędziowe*. Prace naukowe Uniwersytetu Śląskiego w Katowicach, 589.  
 BRAMOWICZ M., KULESZA S., CZAJA P., MAZIARZ W. 2014. *Application of the autocorrelation function and fractal geometry methods for analysis of MFM images*. Archives of Metallurgy and Materials, 59(2): 441–457.

- BRAMOWICZ M., KULESZA S. 2013. *A Magnetic Force Microscopy Study of Magnetic Domain Structure in Maraging Steel*. Solid State Phenomena, 203–204: 315–318.
- DOBRZAŃSKI L.A. 2002. *Podstawy nauki o materiałach i metaloznawstwo*. Wydawnictwo Naukowo-Techniczne, Warszawa.
- MAINSAH E., GREENWOOD J.A., CHETWYND D.G. 2001. *Metrology and Properties of Engineering Surfaces*. Kluwer Academic Publishers.
- SAYLES R., THOMAS T.R. 1978. *Surface topography as a non-stationary random process*. Nature, 271: 431–434.
- WU J.J. 2002. *Analyses and simulation of anisotropic fractal surfaces*. Chaos, Solitons and Fractals, 13: 1791–1806.